Precipitation variations recorded in tree rings from the upper Salween and Brahmaputra River valleys, China

Youping Chen[1, 2], Mary H. Gagen[3], Feng Chen[1, 2], Heli Zhang[2], Huaming Shang[2], Hongfan Xu[1, 2]

1. Yunnan Key Laboratory of International Rivers and Transboundary Eco-Security, Institute of International Rivers and Eco-Security, Yunnan University, Kunming, China

2. Key Laboratory of Tree-ring Physical and Chemic Research of China Meteorological Administration/Key Laboratory of Tree-ring Ecology of Uigur Autonomous Region, Institute of Desert Meteorology, China Meteorological Administration, Urumqi 830002, China

3. Department of Geography, Swansea University, Singleton Park, Swansea, SA2 8PP, UK

ABSTRACT: The spatio-temporal variations of precipitation in the Tibetan Plateau (TP) have vital impacts on fresh water resources, and therefore the sustainable development, over a large part of Asia. Extending instrumental records of precipitation in the regional trans-boundary river basins is critical for resource managers and policy-makers to manage finite water resources in the region under climate change. Here we reconstruct precipitation variations from prior September to current June (r^2 = 43%, 1600-2016 CE) in the upper Salween River valley and from prior July to current April (r^2 = 44%, 1650-2016 CE) in the upper Brahmaputra River valley based on tree ring width variations in conifer tree rings from the Salween and Brahmaputra River basins. Correlation analysis reveals precipitation variations in the two river basins to co-vary over the past 367 years, and a wetting trend is revealed from the 1970s. Spatial correlation analyses with gridded precipitation data extends the reconstruction across the southern Tibetan Plateau. The first eigenvector of our ring

* Corresponding author. Tel.: +86 991 2613017.
E-mail address: feng653@163.com (F. Chen).

width chronologies, and that of other precipitation-sensitive tree ring records from nearby areas successfully captures instrumental streamflow variability in the two river basins. Over the past 3 decades, rapid socio-economic development and population growth in southern and southeastern Asia has pressured the water resource supply of the Tibetan Plateau. Our precipitation reconstructions provide valuable insight for strategies to manage these vital regional water resoures

Keywords: Tree rings; Precipitation reconstruction; Salween River; Brahmaputra River; Water resources management; Tibetan Plateau

1. Introduction

Water resources in the trans-boundary rivers of the southern Tibetan Plateau (TP), are known to be highly sensitive to climate change (Kang et al., 2010; Miller et al., 2012; Cook et al., 2013; Zhang et al., 2013; Li et al., 2013; Lutz et al., 2014; Luo et al., 2014) even based on relatively short (30-60 year) instrumental records. In this important agricultural area runoff is vital for the agricultural water supply, electricity generation and the wider functioning of the river basin (Archer and Fowler, 2004; Bookhagen and Burbank, 2010; Immerzeel et al., 2010; Nepal and Shrestha, 2015). Two important trans-boundary rivers, the Salween and Brahmaputra play an important role in suppling fresh water for China and neighboring countries. Changes in river flow can have potentially extensive geopolitical consequences, because hydrological changes have a profound impact on human settlements and ecosystems in the region. (Gain and Wada, 2014; He et al., 2014; Nepal and Shrestha, 2015). It is important to assess past variability in TP river flow in order to improve our understanding of the wider Asian hydroclimate issues relevant to this region. Our understanding of past climate variability within the trans-boundary river basins is profoundly limited by the short instrumental climate and streamflow records and sparse spatial distribution of weather and streamflow gauge stations in the Tibetan Plateau.

Climate-sensitive tree-ring time series can provide additional data for paleoenvironmental analysis via climate reconstructions (Fritts, 1976). In recent years, many hydroclimate-sensitive tree-ring chronologies have been developed in the trans-boundary river basins of the TP which record both the regional and large-scale hydroclimatic variability that relates to the long-term climate history of interest and importance (Fang et al. 2010; Buckley et al., 2010; D'Arrigo et al., 2011; Sano et al., 2012; Gou et al. 2013; Cook et al. 2013; Zhang et al., 2015; Xu et al., 2015; Hochreuther et al. 2016; Grießinger et al. 2017; He et al. 2017; Xiao et al., 2017). However, there are still many source areas that lack precipitation data and that can only be explored via climate reconstruction. Due to the high spatio temporal variability in regional precipitation is it important to extend the spatial range of tree ring based climate reconstructions to provide the regionally resolved long term picture of hydroclimate needed. Of the TP source areas, the Salween and Brahmaputra Rivers are two of the most important geographical data gaps. Expanding the geographical range of dendroclimate reconstructions also calls for an investigation of new target species. Most of the hydroclimate reconstructions in the southern TP are based on the tree-ring widths of juniper trees (Liu et al., 2011; Zhang et al., 2015; He et al. 2017; Xiao et al., 2017). The cold-temperate coniferous forests that cover the subalpine vegetation zone of the southern TP from 3500 m a.s.l. up to the upper treeline are co-dominated by Juniper (*Juniperus tibetica*), fir (*Abies georgei*), spruce (*Picea likiangensis*) and larch species (*Larix griffithiana*). Juniper trees are mainly distributed near the upper tree lines with low canopy density, while larch and spruce are mainly distributed in river valleys and sub-alpine areas with relatively high canopy density. Here we explore the tree ring reconstruction potential in the coniferous forest belt but extend our target species to include both *Juniperus tibetica* and *Larix griffithiana*, within the upper Salween and Brahmaputra River basins. Inclusion of the coniferous forest species will increase the range and spatial extent of tree ring reconstruction potential for the TP region. We examine the links between precipitation and observed streamflow, and explore mechanisms for streamflow variation control against a background of changing climate.

2. Materials and methods

2.1 Study region and tree-ring data

The Salween and the Brahmaputra Rivers originate from the Tanggula and Himalayan mountains in the southern TP, respectively. Due to the influences of the Asian monsoon, precipitation in the southern TP plays a very important role in the Asian hydrological cycle (Yang et al., 2014). Monsoonal air masses from the Bay of Bengal bring abundant moisture to the southern TP during the summer (JJA) months, whereas continental air masses (in the Asian winter monsoon) lead to dry and cold conditions in the winter (Bräuning and Mantwill, 2004). According to the instrumental climate data, from the Biru climate station (Fig. 1) in the valley of the upper Salween River, the annual mean temperature of the region is 3.7 °C, with the lowest monthly mean temperature of –6.6 °C in January and highest monthly mean temperature of 12.6 °C in July (Fig. 2). The annual total precipitation is 598.7 mm, with precipitation during the warm season (May to September) accounting for 87% of the total annual precipitation. At the Jiali meteorological station, near the valley of the upper Brahmaputra River, the annual mean temperature is -0.3 °C, with the lowest monthly mean temperature of –11.0 °C in January and the highest monthly mean temperature of 8.9 °C in July. Annual total precipitation is 721.5 mm, with precipitation during the warm season (May to September) accounting for 83% of the total annual precipitation (Fig. 2). The two local climate stations reveal the annual precipitation cycle of the upper Salween and Brahmaputra River valleys to be dominated by the Asian summer monsoon (Bräuning and Mantwill, 2004; Su et al., 2016)

Juniper (*Juniperus tibetica*) were sampled at three sites (known as Biribai1-3, hereafter BRB1, BRB2 and BRB3) in the valley of upper Salween River. Larch (*Larix griffithiana*) were sampled at the Jialiluo (hereafter JLL) site in the valley of upper Brahmaputra River (Fig. 1). Both sites are relatively undisturbed by management or other human activity. Trees with the largest diameters, and cylindrical stems, without obvious signs of injury, disease or human disturbance, were selected for sampling. Two increment cores were extracted, coring at breast height from each tree, along different sides of each tree, parallel to slope angle, using standard dendrochronological methods (Stokes and Smiley, 1968). All sampling was carried out in open stands and with trees growing on thin or rocky soils.

Core samples were air dried and mounted and the surface of each core sanded to reveal the ring growth. Ring widths were measured via a LINTAB 6 measuring system with a resolution of 0.001 mm, and the quality of cross-dating checked using the dendrochronological programme COFECHA (Holmes, 1983). Cross-dated tree ring width series were standardized using the program ARSTAN (Cook, 1985) to remove non-climatic trends. Negative exponential functions were used to fit the growth trend for most ring-width series. This conservative method allowed the average age trend in the time series to be removed, whilst applying a conservative approach to maximise the retention of common climatic information. Series whose growth trends could not be described as negative exponential were standardized via the Friedman super-smoothing method (e.g. Gou et al., 2013). Since a high between-tree correlation ($r > 0.6$) was found at the three sites, based on the statistical results of the COFECHA program, all detrended data from the individual juniper trees were combined to develop a longer and replicated regional chronology (at the BRB sites) using a bi-weight robust mean. 129 cores were ultimately used to construct the BRB chronology, of which only two were detrended with the Friedman super-smoothing method (Fig. 3). In the JLL site, 38 larch time series were detrended with negative exponential functions. In order to capture more low frequency signals, we worked with Arstan's STD chronologies for the statistical analyses (see Cook, 1985 for a discussion of Arstan chronology types).

2.2 Dendroclimatic analyses

Monthly average temperature and precipitation data were obtained from the Biru (31.48°N, 93.78°E, 3941 m a.l.s., 1979-2016) and Jiali (30.67°N, 93.28°E, 4490 m a.l.s., 1965-2016) weather stations (Fig. 1; Table 1). Simple linear correlations between the standard tree ring width chronologies (BRB and JLL) and instrumental climate data were investigated with a response function approach (Biondi and Waikul, 2004), exploring correlations with monthly climate averages from July of the previous growth year through September of the current year. Furthermore, in order to select the most appropriate predictands for climate reconstructions, we also screened the standard chronologies via correlation analysis with seasonal climate combinations.

Our simple linear response function analysis revealed strong negative correlations with May-

June temperatures from the Biru station and positive correlations for total (previous) September- (current) June precipitation and total (previous) July- (current) April precipitation at the Jiali station (Fig. 4). This is logical as it indicates that warm temperatures in the current year accelerate the pre-monsoon drought, and on the contrary, high rainfall from winter and concurrent early spring satisfies the water demand of the earlywood ring growth. Further, Pearson correlation analysis revealed strongest correlations with total (previous) September- (current) June Biru precipitation and total (previous) July- (current) April Jiali precipitation. Based on the significant correlations between seasonal combinations of precipitation and the ring width chronologies, we established linear regression models for the precipitation reconstructions. Due to the relatively short climate observation data in the study area, the leave-one-out cross-validation method (Michaelsen, 1987) was used to assess the reliability of the reconstruction models.

To indicate that our reconstructions reflected regional-scale precipitation variations, we explored correlations between the tree ring time series and gridded climate data (the CRU precipitation dataset) (Harris et al., 2014). In order to explore possible driving forces behind regional precipitation variability we calculated the spatial correlations between ring with chronologies and a sea surface temperature data set (HadISST, Rayner et al., 2003). To assess the impact of regional precipitation on runoff, we used principal component analysis (PCA) to extract the common signals from our chronologies and a wider network of precipitation-sensitive sites in southern TP.

3. Results

3.1 Tree ring width chronologies and their relationship with climate factors

The results of a statistical analysis using simple linear correlation to explore the tree-ring width chronologies of juniper and larch are presented in Table 2. The mean segment length of the chronologies are 175 years (BRB) and 228 years (JLL), respectively. Based on the subsample signal strength (SSS ⩾ 0.85, Buras, 2017) and sample replication (⩾ 3 trees), the chronologies are considered to have an acceptably high signal to noise ratios after 1600 CE for BRB and 1650 CE for JLL. The juniper and larch chronologies showed relatively low year-to-year variations (MS, range from 0.19 to 0.23), which is typical for conifers trees growing in the relatively humid environments of river valleys (Fritts, 1976). High correlations with the master series, variance in the first eigenvector and SSS indicate that the juniper and larch chronologies contain strong common signals and are thus suitable for the dendroclimatic analysis (Table 2).

The BRB ring-width chronologies are significantly positively correlated with precipitation in the previous September, and concurrent May and June, and negatively correlated with temperature from concurrent year May to June (Fig. 4). These relationships are similar to results from previous studies (Zhang et al., 2015; He. 2018), and indicate that the drought forcing of the pre-monsoon season is the primary climatic factor that controls radial juniper growth, analogous with other studies from the southern TP. After calculating the correlations between the BRB ring-width chronology and different seasonal climate combinations, the highest correlation between tree rings and seasonal precipitation was found in September–June ($r = 0.655$; $p < 0.001$), correlations between tree-ring widths and total July–June precipitation were also high ($r = 0.608$; $p < 0.001$), suggesting that tree ring widths of the upper Salween River juniper provide a reliable indicator of precipitation changes in the valley.

For the JLL site, ring-width indices of the larch trees are significantly positively correlated with precipitation in prior August and September, and negatively correlated with temperature from prior November to December (Fig. 4). The climate correlations in the current year are much lower for at the JLL site but correlations with previous year August-September precipitation are high. Following the calculation of single month correlations, correlations between the ring-width indices and different seasonal combinations were explored. The highest correlation ($r = 0.664$; $p < 0.001$) was found between JLL ring widths and July (previous) to April (concurrent year) precipitation. Based on the above climate response analysis, we hypothesise that the limiting factor to the annual ring width growth of larch at the site is cumulative precipitation amount from the summer prior to ring growth, through the summer monsoon season to winter and current early spring.

3.2 Precipitation reconstruction for the valley of the upper Salween River

The highest simple linear correlation ($r = 0.655$) is revealed between the BRB chronology and total (previous) September- (concurrent) June precipitation. Based on the results of the correlation analysis for the valley of the upper Salween River, the total precipitation from prior September to June of the growth year was chosen for reconstruction. The regression model is shown below:

$$P_{BRB} = 167.73BRB + 163.61 \qquad (1)$$

The P_{BRB} regression model is the total (previous) September- (concurrent) June precipitation (61.2% of the total annual precipitation) and BRB is the tree-ring width index for current year (t). During the common period for which we have both tree ring and precipitation data (1979–2016), the reconstruction accounted for 42.9% of the explained variance in the precipitation data (Fig. 5A). As shown in Table 3, product means test statistics and the sign test were found to be statistically significant, and the reduction of error (RE) to be positive.

Based on the linear regression model, we developed a total (previous) September- (concurrent) June precipitation reconstruction from 1600 to 2016 CE for the valley of the upper Salween River (Fig. 6). The long-term mean of total September-June precipitation is 327.9 mm. A 31-year fast Fourier transformation was employed to highlight the decadal-frequency variation of the reconstruction. Five periods (> 10 years), CE 1600-1611, 1708-1720, 1755-1794, 1809-1844 and 1899-1981, showed precipitation levels lower than the 417-year mean, reflecting relatively humid conditions. While notably wet periods occur in the reconstruction at 1612-1645, 1654-1707, 1721-1754, 1795-1808, 1845-1898 and 1982-2016.

3.4 Precipitation reconstruction for the valley of upper Brahmaputra River

Based on the results of the correlation analysis for the upper basin of Brahmaputra River, the total precipitation from prior July to April of the growth year was chosen for reconstruction. The regression model is shown below:

$$P_{JLL} = 207.34JLL + 273.39 \quad (2)$$

The P_{JLL} regression model include the total precipitation of prior July to concurrent April (a time period in which 69.2% of the total annual precipitation falls) and JLL is the tree-ring width index for current year (*t*). The trends also show that actual and reconstructed values match well during the common period from 1965 to 2016 (Fig. 5B), and the explained variance of the full model is 44.1%. The leave-one-out cross-validation test also shows that the precipitation reconstruction model for the valley of upper Brahmaputra River is time stable (Table 3). Based on the linear regression model, we reconstructed total July- April precipitation for the valley of upper Brahmaputra River from 1650 to 2016 (Fig. 5). The long-term mean of total July- April precipitation is 476.4 mm. The 31-year fast Fourier transformation show several significant dry/wet periods: CE 1650-1622, 1691-1711, 1762-1786, 1807-1830, 1842-1851, 1875-1898, 1908-1937 and 1944-1981 were relatively dry and while 1663-1690, 1712-1761, 1787-1806, 1831-1841, 1852-1874 and 1982-2016 were relatively wet. In the recent 30 years, a strong wetting trend is occurred at the valley of the upper Salween and Brahmaputra River.

4. Discussion

4.1 Climate–growth relationships

The climate response analysis indicated that precipitation variation was a major limiting factor for conifer growth in the upper Salween and Brahmaputra River valleys. This relationship resembles other findings in surrounding areas (He et al., 2013; Yang et al., 2014b; Chen et al., 2017) and indicates the importance of previous summer precipitation and winter-early spring snowfall to conifer growth. Conifer growth during the early phase of the growing season is largely supplied by snowmelt from the high mountain, the same water source that recharges soil moisture and streamflow during this period. Dry conditions before the onset of the monsoon season precipitation stress the trees and reduce growth rates and streamflow. Later in the summer, enough monsoonal precipitation is available to satisfy the water demand for tree growth.

Significant negative correlations between May-June temperature and juniper growth were found. Due to surface exposure and low canopy density, high temperatures during May-June enhance evapotranspiration and reduce soil moisture and result in lower radial growth of juniper trees (Zhang et al., 2015). Due to the relatively higher ground cover and canopy density of larch forest the high temperature has relatively little effect on the evaporation of soil water and causes larch to have a relatively low response to temperature during the growing season. Low correlations between tree-ring series of larch and temperature imply that temperature has no little significant influence on larch growth at these sites. Increased November-December temperatures may mean less freezing damage to tree trunk and roots, and thus less growth limitation in the larch trees sampled.

4.2 Regional- to large-scale comparison

The valleys of the upper Salween and Brahmaputra River are located in a similar climate zone, and the straight distance between the BRB and JLL sites is about 40 kilometers. Therefore, despite being different species, it can be expected that the main factor limiting tree growth (precipitation) on the thin or rocky soils of the river valleys should be consistent. Correlations between the two precipitation reconstructions, calculated over the 1650–2016 common period are r=0.33, and increase to r=0.57 after 31-yr smoothing, and the first principal component (PC1) accounts for 66% of the total variance. Spatial correlations with gridded precipitation data showed similar fields for the two precipitation reconstructions and PC1, although correlations were lower for the BRB precipitation reconstruction (Fig. 7). Significant positive correlations with southern TP gridded precipitation data were found, with the highest correlations occurring in the appropriate valleys. The results confirm that our tree-ring records from juniper and larch capture the precipitation variability of the river valleys of the southern TP. Notably high precipitation periods occurred during 1663-1690, 1721-1754, 1795-1806, 1852-1874 and 1982-2016. The periods 1762-1786, 1809-1830, 1908-1937 and 1944-1981 were relatively dry. There were 247 years in the common wet/dry periods in the two basins, accounting for 67% of the total period. Further comparisons between the two precipitation reconstructions reveal that precipitation has increased significantly after the 1970s.

The mean anomaly percentage of the wet period 1663-1690 is +6.1%, 1721-1754 is +8.5%, 1795-1806 is +4.3%, and 1982-2016 is +9.5%. As a result, the upper Salween and the Brahmaputra River Basin have, since the 1970s, experienced an increase in rainfall of note over the last 367 years. This markedly wet period was also reported for the other areas of the upper Brahmaputra River Basin (Liu et al., 2011; He et al., 2012). Regional climate warming may be being modified by this increasing precipitation trend, which may be a reason for the lack of warmer season temperatures in the southern TP over the recent instrumental period (Bräuning and Mantwill, 2004; Lv et al., 2014). Such regional modification of the global average increase in temperature associated with the enhanced greenhouse effect is seen elsewhere, in interactions between regional circulation patterns and global warming (Young et al., 2019). Some differences existing between the two reconstructions may reflect the influences of spatial difference in local precipitation and tree growth in the complex mountain terrain or differences in the seasonality of tree growth.

We review other precipitation-sensitive tree-ring records in the surrounding region. A precipitation reconstruction was established with *Picea likiangensis* in northeastern Tibet by Shang et al. (2018), with *Abies forrestii* in west Sichuan on the TP by Gou et al. (2013) and Li et al. (2017). Based on tree-ring data of *Juniperus tibetica*, total July-June precipitation and NDVI reconstructions were developed for the Lhasa river valley (He et al., 2013; Shang et al., 2016). Correlations between our first mode of variability (PC1) and Shang et al. (2016), Shang et al. (2018), Li et al. (2017), computed over the 1650–2011 common period are 0.42, 0.35 and 0.20 ($P < 0.001$), and suggesting multiple tree species of the river valley of southern TP show sensitivity to modes of climate variability related to pre monsoon conditions. This lays the foundation for exploring large-scale climate modes of interest from these reconstructions

Based on the tree-ring data of juniper trees, Zhang et al. (2015) reconstruct May-June PDSI of the TP during the past 500 years, revealing the influences on drought variations within the TP of interactions between the Asian summer monsoon and the westerlies. We use the most representative annual precipitation reconstruction sequence in the northern TP (Yang et al., 2014b) to compare with our PC1 to further probe these relationships. The correlation between the original reconstructions is 0.19 (p < 0.001). After smoothing with a 31-year moving average, significantly differences in the low-frequency signals were found between precipitation in the southern and northern parts of the TP (Fig. 8). The out-of-phase relationships between the series also supports a connection between the Asian summer monsoon and the westerlies. Meanwhile, the two sequences also indicated that there was a significant increase in precipitation throughout the TP in the past 30 years, in agreement with the post 1970 wetter phase in our reconstructions. The mechanism by which the interaction between regional circulation patterns and large-scale atmospheric circulation systems (Asian summer monsoon and the westerlies) control regional precipitation variations in the context of warming awaits further investigation.

4.3 Linkages with climate changes

A significant negative correlation is seen between proxy PC1 and SSTs (HadISST) in the equatorial Indian and eastern Pacific Ocean during the period 1960-2011 suggesting a possible teleconnection with El Niño/Southern Oscillation (ENSO) (Fig. 9). Our PC1 also has significant correlations with SSTs in the northern Indian Ocean and western Pacific Ocean suggestive of the impacts of the Asian summer monsoon on precipitation in our study region. Previous studies have indicated that negative (positive) ENSO and Indian Ocean Dipole (IOD) episodes, occurring in years of extreme wetness (dryness) on the Tibetan plateau, tend to be concomitant with strong (weak) summer monsoon phases (Jia and Zhou, 2003; Bothe et al., 2010; Chen et al., 2019). During cold ENSO years, strong southwesterly flow occurs over western-central Tibet and Pakistan. This strong southwesterly monsoon advects water vapor from the Bay of Bengal and Arabian Sea leading to increased precipitation, and vice versa (Chen et al., 2019). The correlations between our proxy PC1 and SST in the equatorial western Indian and eastern Pacific Ocean support such a connection. Meanwhile, a weakening Asian monsoon has been observed since late 1970s, and has some significant influences with precipitation changes in monsoon Asia (Wang, 2001; Li and Zeng, 2002). However, the precipitation rate of our study area increased by 0.48 mm/a in May, 0.14 mm/a in June, -0.28 mm/a in July, 0.04 mm/a in August and 0.06 mm/a in September from 1980 to 2016, and suggests the precipitation in the river valleys increased significantly in spring. During the pre-monsoon season, precipitation is relatively low. Warm and dry conditions before the onset of the monsoon season cause water stress for the earlywood growth and lead to a strong response of tree growth to precipitation variability (Zhang et al., 2015). As shown by instrumental climate and tree-ring data (Fan et al., 2008; Zhang et al., 2015; Li et al., 2017; Yadav et al., 2017), spring precipitation increased in southern TP and surrounding areas, and thus, tree-growth, benefit from the spring precipitation. Increased precipitation in spring may be linked to the accelerated water cycle and early start of the rainy season in the context of global warming (Ueda and Yasunari, 1998; Tamura et al., 2010). These findings suggesting that precipitation variation in southern TP has strong linkages with large-scale ocean–atmosphere–land circulations.

4.4 Linkages with streamflow of the Salween and Brahmaputra River

Precipitation is the main water source for the Salween and Brahmaputra river basins (rather than snow melt) (Immerzeel, 2008; Wang and Chen, 2017; Chen et al., 2018). Thus, understanding past precipitation changes is important for estimating water resource conditions in the basins of the wider region. Although the distance between the Daojieba hydrographic station (24.98°N, 98.80°E, 685m a.s.l.) (Salween river) and Yangcun hydrographic station (Brahmaputra river) (91.82°E, 29.26°N, 3550 m a.s.l) is over 750 km (Fig. 1; Table 1) the instrumental streamflow records are significantly correlated (r = 0.73, p< 0.001) over the common period, suggesting that the hydroclimate of the Southern TP influences streamflow across a wide region of this part of southern Asia. Based on these positive instrumental period correlations, we explored the combined analysis of precipitation-sensitive tree-ring records from this study and Shang et al., (2016), (2018) and Li et al., (2017). The records were merged via PCA to form the first principal component containing 42% of the total series variance. This new predictor contains 36% of the total variance of the sum of flow data from two stations, giving us confidence that the streamflow of the Salween and Brahmaputra basins can be preliminarily compared to the variability in the tree-ring records. Based on the tree-ring records, the average annual runoff was 81.5 billion cubic meters from the two stations during the past three centuries, and the runoff (> 4.6%) has shown an upward trend during the last 30 years, in line with the changes in regional precipitation discussed above. Although the lower reaches of the two rivers belong to the monsoon climate belt, with relatively abundant precipitation, drought events are related to periodic monsoon failures in the region (Cook et al., 2010). Compared with the results of a large scale tree-ring based Asian monsoon drought reconstruction (The Monsoon Asian Drought Atlas – MADA - Cook et al., 2010), we found that some dry periods in the downstream countries are synchronized with the streamflow reduction from southern TP, such as the mid–18th-century MADA Strange Parallels drought, late Victorian great drought and Bengal Famine 1943-1945, which have led to the deaths of thousands of people (Padmanabhan, 1973; Cook et al., 2010) (Fig. 9). Due to the sparse population in the TP, the impact of drought and low streamflow on society are relatively small. The lower river basin areas are significantly more populous, and such synchronization of extreme drought events would have a significant impact on the socio-economic development of the downstream countries. Therefore, for the sustainable development of all countries in the two river basins, it is necessary to develop more effective and reasonable water resource allocation mechanism.

5. Conclusions

Based on our *Juniperus tibetica* and *Larix griffithian* derived tree ring chronologies from the valleys of upper Salween and Brahmaputra River, we reconstructed total September-June precipitation in the valley of upper Salween River from 1600 CE and total July-April precipitation in the valley of upper Brahmaputra River from 1650 CE, respectively. The two precipitation reconstructions are consisten, and indicate that a wetting trend has occurred in the valleys of the upper Salween and Brahmaputra Rivers since the 1970s. Comparison with other precipitation-sensitive tree-ring records shows high coherency across the southern TP. As a result, we further used tree-ring data to assess the water supply of these two rivers over the past three centuries and have found that widespread droughts and the resulting reduction in runoff can have some important impacts.

Our results are of particular interest as the TP is one of the main fresh water sources for the downstream areas in large parts of southern Asia. Over the past 30 years, rapid socio-economic development and human population growth in southern and southeastern Asia raises doubts over the stability of the water resource supply of TP to meet the growing needs of the downstream areas. The relationships between the tree rings and precipitation/streamflow presented for southern TP are an encouraging indication of the potential for dendrohydrology research in TP. All scenarios presented in the precipitation reconstruction provide valuable insight for strategies to understand changing climate and water resources in the region. The information provided herein on past hydrological variation should prove of much interest to government regulators and researchers concerned with hydrological forecasts, water resource plans, and other applications.

Acknowledgments

This work was supported by the National Key R&D Program of China (2016YFA0601600), NSFC (91547115 and U1803341) and the national youth talent support program. We thank the reviewers very much whose comments greatly benefitted this manuscript.

References

Archer, D. R., Fowler, H. J. (2004). Spatial and temporal variations in precipitation in the Upper Indus Basin, global teleconnections and hydrological implications. Hydrology and Earth System Sciences Discussions, 8(1), 47-61.

Biondi, F., Waikul, K. (2004). DENDROCLIM2002: A C + + program for statistical calibration of climate signals in treering chronologies. Computers & Geosciences 30, 303-311.

Bräuning, A., Mantwill, B. (2004). Summer temperature and summer monsoon history on the Tibetan plateau during the last 400 years recorded by tree rings. Geophysical Research Letters, 31(24).

Bookhagen, B., Burbank, D. W. (2010). Toward a complete Himalayan hydrological budget: Spatiotemporal distribution of snowmelt and rainfall and their impact on river discharge. Journal of Geophysical Research: Earth Surface, 115(F3).

Bothe, O., Fraedrich, K., Zhu, X. (2010). The large ‐ scale circulations and summer drought and wetness on the Tibetan plateau. International Journal of Climatology, 30(6), 844-855.

Buckley, B. M., Anchukaitis, K. J., Penny, D., Fletcher, R., Cook, E. R., Sano, M., Nam, L., Wichienkeeo, A., Minh, T.T., Hong, T. M. (2010). Climate as a contributing factor in the demise of Angkor, Cambodia. Proceedings of the National Academy of Sciences, 107(15), 6748-6752.

Buras, A. (2017). A comment on the expressed population signal. Dendrochronologia, 44, 130-132.

Chen, F., Yuan, Y., Yu, S.L. (2017). Tree-ring indicators of rainfall and streamflow for the Ili-Balkhash Basin, Central Asia since CE 1560. Palaeogeography, Palaeoclimatology, Palaeoecology, 482: 48-56.

Chen, F., Yuan, Y., Fan, Z., Yu, S. (2018). A Winter Precipitation Reconstruction (CE 1810–2012) in the Southeastern Tibetan Plateau and Its Relationship to Salween River Streamflow Variations. Pure and Applied Geophysics, 175, 2279–2291.

Chen, F., Shang, H., Panyushkina, I. P., Meko, D. M., Yu, S., Yuan, Y., Chen, F. (2019). Tree-ring reconstruction of Lhasa River streamflow reveals 472 years of hydrologic change on southern Tibetan Plateau. Journal of Hydrology, 572, 169-178

Cook, E. R., 1985. A time series analysis approach to tree ring standardization. Dissertation for the Doctoral Degree. Arizona: The University of Arizona.

Cook, E. R., Palmer, J. G., Ahmed, M., Woodhouse, C. A., Fenwick, P., Zafar, M. U., Wahab, M., Khan, N. (2013). Five centuries of Upper Indus River flow from tree rings. Journal of Hydrology, 486, 365-375.

Cook, E. R., Anchukaitis, K. J., Buckley, B. M., D’Arrigo, R. D., Jacoby, G. C., Wright, W. E. (2010). Asian monsoon failure and megadrought during the last millennium. Science, 328(5977), 486-489.

Cuo, L., Zhang, Y., Zhu, F., Liang, L. (2014). Characteristics and changes of streamflow on the Tibetan Plateau: a review. Journal of Hydrology: Regional Studies, 2, 49-68.

D'Arrigo, R., Palmer, J., Ummenhofer, C. C., Kyaw, N. N., Krusic, P. (2011). Three centuries of Myanmar monsoon climate variability inferred from teak tree rings. Geophysical Research Letters, 38(24).

Fan, Z. X., Bräuning, A., Cao, K. F. (2008). Tree-ring based drought reconstruction in the central Hengduan Mountains region (China) since AD 1655. International Journal of Climatology, 28(14), 1879-1887.

Fang, K., Gou, X., Chen, F.H, Li, J.B., D'Arrigo, R.D., Cook, E., Yang, T., Davi, N. (2010). Reconstructed droughts for the southeastern tibetan plateau over the past 568 years and its linkages to the pacific and atlantic ocean climate variability. Climate Dynamic, 35(4), 577-585.

Fritts, H.C., 1976. Tree Rings and Climate. Academic Press, New York, 567pp.

Gain, A. K., Wada, Y. (2014). Assessment of future water scarcity at different spatial and temporal scales of the Brahmaputra River Basin. Water resources management, 28(4), 999-1012.

Gou, X., Yang, T., Gao, L., Deng, Y., Yang, M., Chen, F. (2013). A 457-year reconstruction of precipitation in the southeastern Qinghai-Tibet Plateau, China using tree-ring records. Chinese Science Bulletin, 58(10), 1107-1114.

Grießinger, J., Bräuning, A., Helle, G., Hochreuther, P., Schleser, G. (2017). Late Holocene relative humidity history on the southeastern Tibetan plateau inferred from a tree-ring δ18O record: Recent decrease and conditions during the last 1500 years. Quaternary International, 430, 52-59.

Harris, I. P. D. J., Jones, P. D., Osborn, T. J., Lister, D. H., 2014. Updated high-resolution grids of monthly climatic observations–the CRU TS3. 10 Dataset. International Journal of Climatology, 34(3), 623-642.

He, D., Wu, R., Feng, Y., Li, Y., Ding, C., Wang, W., Douglas, W. Y. (2014). China's transboundary waters: new paradigms for water and ecological security through applied ecology. Journal of Applied Ecology, 51(5), 1159-1168.

He, M., Yang, B., Bräuning, A., Wang, J., Wang, Z. (2013). Tree-ring derived millennial precipitation record for the south-central Tibetan Plateau and its possible driving mechanism. The Holocene, 23(1), 36-45.

He, M., Bräuning, A., Grießinger, J., Hochreuther, P., Wernicke, J. (2018). May–June drought reconstruction over the past 821 years on the south-central Tibetan Plateau derived from tree-ring width series. Dendrochronologia, 47, 48-57.

Holmes, R. L. (1983). Computer-assisted quality control in treering dating and measurement. Tree-Ring Bulletin, 44, 69-75.

Hochreuther, P., Wernicke, J., Grießinger, J., Mölg, T., Zhu, H., Wang, L., Bräuning, A. (2016). Influence of the Indian Ocean Dipole on tree-ring δ18O of monsoonal Southeast Tibet. Climatic Change, 137(1-2), 217-230.

Immerzeel, W. (2008). Historical trends and future predictions of climate variability in the Brahmaputra basin. International Journal of Climatology, 28(2), 243-254.

Immerzeel, W. W., Van Beek, L. P., Bierkens, M. F. (2010). Climate change will affect the Asian water towers. Science, 328(5984), 1382-1385.

Jia, L., Zhou, S.W., 2003. The effect of Indian Ocean SST anomaly on Indian Monsoon and summer precipitation over Tibetan Plateau. Plateau Meteorol. 22, 132–137.

Kang, S., Xu, Y., You, Q., Flügel, W. A., Pepin, N., Yao, T. (2010). Review of climate and cryospheric change in the Tibetan Plateau. Environmental Research Letters, 5(1), 015101.

Li, J., Zeng, Q. (2002). A unified monsoon index. Geophysical Research Letters, 29(8), 115-1.

Li, F., Zhang, Y., Xu, Z., Teng, J., Liu, C., Liu, W., Mpelasoka, F. (2013). The impact of climate change on runoff in the southeastern Tibetan Plateau. Journal of Hydrology, 505, 188-201.

Li, J., Shi, J., Zhang, D. D., Yang, B., Fang, K., Yue, P. H. (2017). Moisture increase in response to high-altitude warming evidenced by tree-rings on the southeastern Tibetan Plateau. Climate Dynamics, 48(1-2), 649-660.

Liu, J., Yang, B., Qin, C. (2011). Tree-ring based annual precipitation reconstruction since AD 1480 in south central Tibet. Quaternary International, 236(1-2), 75-81.

Lutz, A. F., Immerzeel, W. W., Shrestha, A. B., Bierkens, M. F. P. (2014). Consistent increase in High Asia's runoff due to increasing glacier melt and precipitation. Nature Climate Change, 4(7), 587.

Xing, P., Zhang, Q. B., Lv, L. X. (2014). Absence of late-summer warming trend over the past two and half centuries on the eastern Tibetan Plateau. Global and Planetary Change, 123, 27-35.

Michaelsen, J. (1987). Cross-validation in statistical climate forecast models. Journal of climate and Applied Meteorology, 26(11), 1589-1600.

Miller, J. D., Immerzeel, W. W., Rees, G. (2012). Climate change impacts on glacier hydrology and river discharge in the Hindu Kush–Himalayas: a synthesis of the scientific basis. Mountain Research and Development, 32(4), 461-467.

Nepal, S., Shrestha, A. B. (2015). Impact of climate change on the hydrological regime of the Indus, Ganges and Brahmaputra river basins: a review of the literature. International Journal of Water Resources Development, 31(2), 201-218.

Padmanabhan, S. Y. (1973). The great Bengal famine. Annual Review of Phytopathology, 11(1), 11-24.

Rayner, N. A., Parker, D. E., Horton, E. B., Folland, C. K., Alexander, L. V., Rowell, D. P., Kent, E. C., Kaplan, A. (2003). Global analyses of sea surface temperature, sea ice, and night marine air temperature since the late nineteenth century. Journal of Geophysical Research: Atmospheres, 108(D14).

Sano, M., Xu, C., Nakatsuka, T. (2012). A 300-year Vietnam hydroclimate and ENSO variability record reconstructed from tree ring δ18O. Journal of Geophysical Research: Atmospheres, 117(D12).

Shewale, M.P., Kumar, S. Climatological features of drought incidences in India. Meteorological Monograph (Climatology 21/2005). National Climate Centre, Indian Meteorological Department, 2005.

Shang, H.M., Wei, W.S., Yuan, Y.J., Yu, S.L., Zhang, R.B., Hong, J.C., Chen, F., Zhang, T.W., Fan, Z.A. (2016). Normalized vegetation variation index reconstruction based on the tree-ring width in central Tibet. Journal of Lanzhou University: Natural Sciences, 52(1), 18-24.

Shang, H.M., Hong, J.C., Zhang, R.B., Fan, Z.A., Chen, F. (2018). Tree-ring recorded 522-year precipitation from previous October to May in northeastern Tibet, China. Mountain Research, 36: 661-668.

Stokes, M. A., Smiley, T. L. (1968). An Introduction to Tree-Ring Dating. University of Chicago Press, 73 pp.

Su, F., Zhang, L., Ou, T., Chen, D., Yao, T., Tong, K., Qi, Y. (2016). Hydrological response to future climate changes for the major upstream river basins in the Tibetan Plateau. Global and Planetary Change, 136: 82-95.

Tamura, T., Taniguchi, K., Koike, T. (2010). Mechanism of upper tropospheric warming around the Tibetan Plateau at the onset phase of the Asian summer monsoon. Journal of Geophysical Research: Atmospheres, 115(D2).

Ueda, H., Yasunari, T. (1998). Role of warming over the Tibetan Plateau in early onset of the summer monsoon over the Bay of Bengal and the South China Sea. Journal of the Meteorological Society of Japan. Ser. II, 76(1), 1-12.

Wang, H.J. (2001). The weakening of the Asian monsoon circulation after the end of 1970's. Advances in Atmospheric Sciences, 18(3), 376-386.

Wang, H., Chen, F. (2017). Increased stream flow in the Nu River (Salween) Basin of China, due to climatic warming and increased precipitation. Geografiska Annaler: Series A, Physical Geography, 99(4), 327-337.

Wigley, T. M., Briffa, K. R., Jones, P. D. (1984). On the average value of correlated time series, with applications in dendroclimatology and hydrometeorology. Journal of climate and Applied Meteorology, 23(2), 201-213.

Xiao, D., Shao, X., Qin, N., Huang, X. (2017). Tree-ring-based reconstruction of streamflow for the Zaqu River in the Lancang River source region, China, over the past 419 years. International Journal of Biometeorology, 61(7), 1173-1189.

Xu, C., Pumijumnong, N., Nakatsuka, T., Sano, M., Li, Z. (2015). A tree-ring cellulose δ18O-based July–October precipitation reconstruction since AD 1828, northwest Thailand. Journal of Hydrology, 529, 433-441.

Yang, K., Wu, H., Qin, J., Lin, C., Tang, W., Chen, Y. (2014). Recent climate changes over the Tibetan Plateau and their impacts on energy and water cycle: A review. Global and Planetary Change, 112, 79-91.

Yang, B., Qin, C., Wang, J., He, M., Melvin, T. M., Osborn, T. J., Briffa, K. R. (2014b). A 3,500-year tree-ring record of annual precipitation on the northeastern Tibetan Plateau. Proceedings of the National Academy of Sciences, 111(8), 2903-2908.

Yadav, R. R., Gupta, A. K., Kotlia, B. S., Singh, V., Misra, K. G., Yadava, A. K., Singh, A. K. (2017). Recent wetting and glacier expansion in the northwest Himalaya and Karakoram. Scientific reports, 7(1), 6139.

Young, G. H., Gagen, M. H., Loader, N. J., McCarroll, D., Grudd, H., Jalkanen, R., Kirchhefer, A., Robertson, I. (2019). Cloud cover feedback moderates Fennoscandian summer temperature changes over the past 1000 years. Geophysical Research Letters, doi: 10.1029/2018GL081046.

Zhang, L., Su, F., Yang, D., Hao, Z., Tong, K. (2013). Discharge regime and simulation for the upstream of major rivers over Tibetan Plateau. Journal of Geophysical Research: Atmospheres, 118(15), 8500-8518.

Zhang, Q. B., Evans, M. N., Lyu, L. (2015). Moisture dipole over the Tibetan Plateau during the past five and a half centuries. Nature Communications, 6, 8062.

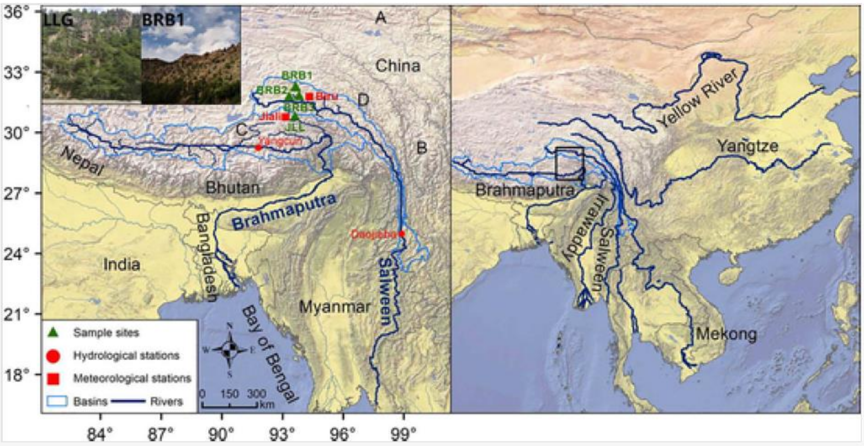

Location of the sampling sites, weather stations (Biru and Jiali) and hydrologic stations (Yangcun and Daojieba) in the upper Salween and Brahmaputra River. The A, B, C, D and E denote the tree ring sites of Yang et al. (2014b), Li et al. (2017), Shang et al. (2016) and Shang et al. (2018), respectively.

Fig. 2

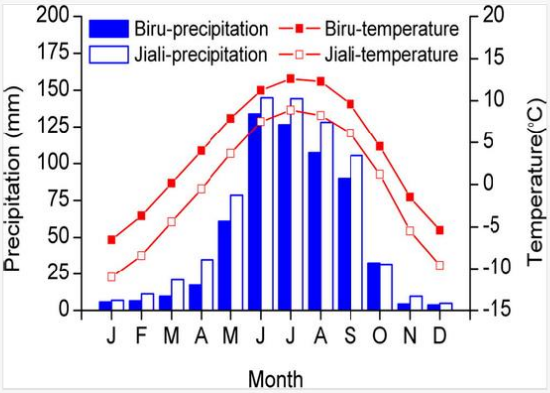

Monthly total precipitation and mean temperature at the Biru (1979–2016) and Jiali (1966–2016) climate stations.

Fig. 3

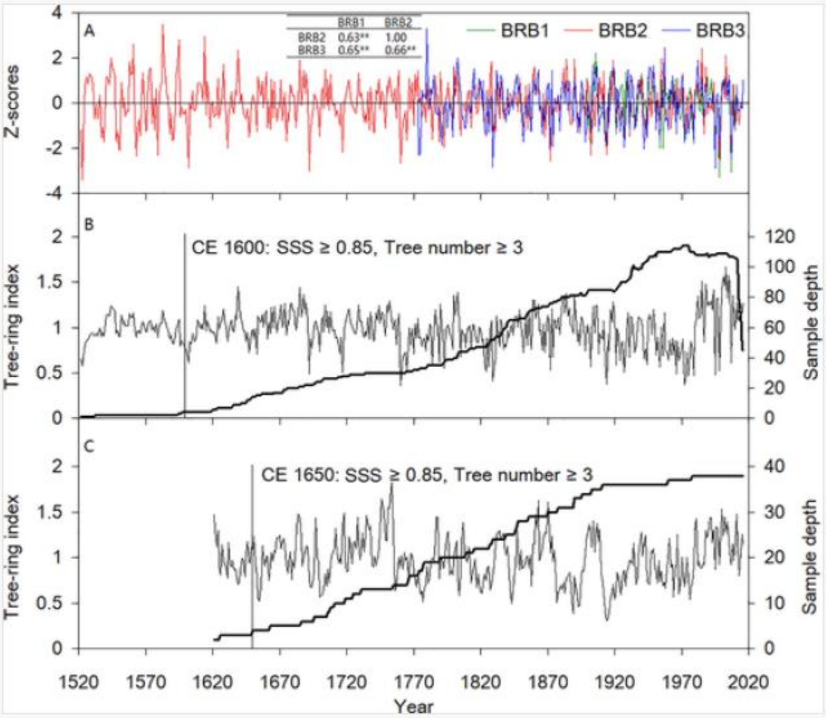

(A) The master cross-dating series of BRB1, BRB2 and BRB3 from the software Cofecha. (B) Plot of the standard juniper chronology from the valley of upper Brahmaputra River, and its reliable period and the sample depth. (C) Plot of the standard juniper chronology from the valley of upper Salween River, and its reliable period and the sample depth.

Table 1

Site information for the sampling sites, weather stations and hydrological stations (see Fig. 1).

Site	Lat. (N)	Long. (E)	Elevation (m)	Aspect	Slope	canopy density	Tree number	Species
BRB1	31.76°	93.61°	4159	SE	40°–45°	0.1	17	*Juniperus tibetica*
BRB2	31.57°	93.60°	4400	SE	20–40°°	0.1	22	*Juniperus tibetica*
BRB3	31.54°	93.39°	4136	SE	20–40°	0.1	30	*Juniperus tibetica*
JLL	30.60°	93.66°	4090	S	20–30°	0.1–0.3	19	*Larix griffithiana*
Biru	31.48°	93.78°	3941					
Jiali	30.67°	93.28°	4490					
Yangcun	29.47°	94.65°	3080					
Daojieba	24.98°	98.80°	685					

Fig. 4

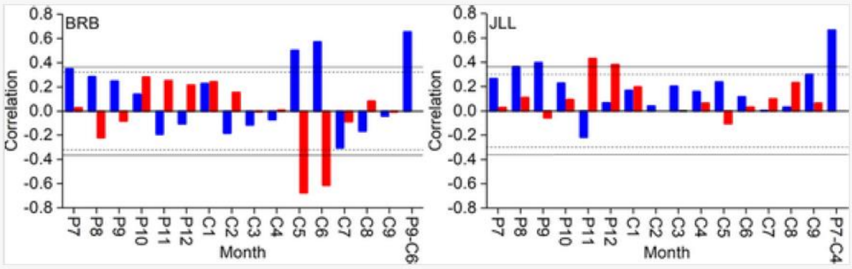

The correlation between ring-width indices and monthly total precipitation (blue bars) and monthly mean temperature (red bars). Meteorological data come from Biru (BRB) and Jiali (JLL). Horizontal dashed lines are the 95% confidence level. Horizontal outer lines are the 99% confidence level.

Table 2

Parameter	BRB	JLL
Mean sensitivity	0.182	0.168
Standard deviation	0.208	0.262
Signal to noise ratio	59.859	20.715
Mean correlation with master series	0.619	0.629
Variance in first eigenvector	49.2%	41.4%
Expressed Population Signal	0.984	0.954

Fig. 5

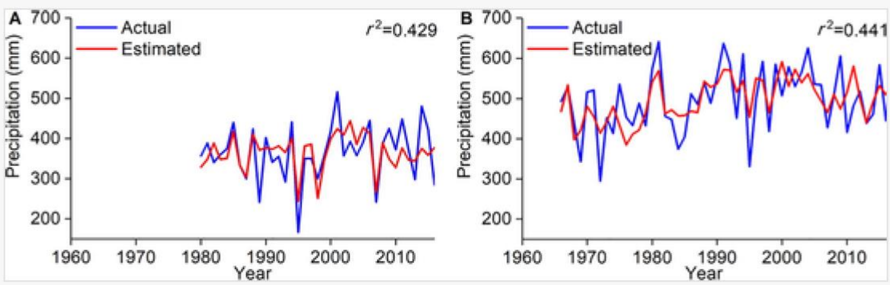

Comparison between observed and estimated precipitation for the valleys of the Salween (A) and the Brahmaputra River (B).

Table 3

Leave-one-out cross-validation statistics for the two precipitation reconstructions for the river valleys of the southern TP based on tree-ring data.

Verification	BRB	JLL
r	0.598	0.624
r^2	0.358	0.389
RE	0.481	0.496
PMT	2.966	4.243
Sign test	$27^+/12^-$	$40^+/11^-$

Fig. 6

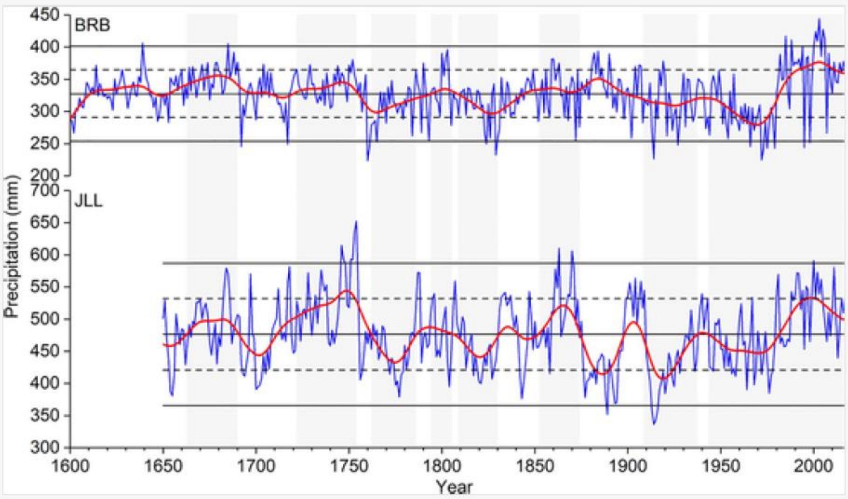

Reconstructed total September–June precipitation for the Salween River Basin (BRB) and total July-April precipitation for the Brahmaputra River Basin (JLL). The red line was smoothed with a 31-year FFT (fast Fourier transform) filter. The central horizontal line shows the mean of the estimated values; inner horizontal (dotted) lines show the border of one standard deviation, and outer horizontal lines show two standard deviations. The shadow means the common wet/dry periods.

Fig. 7

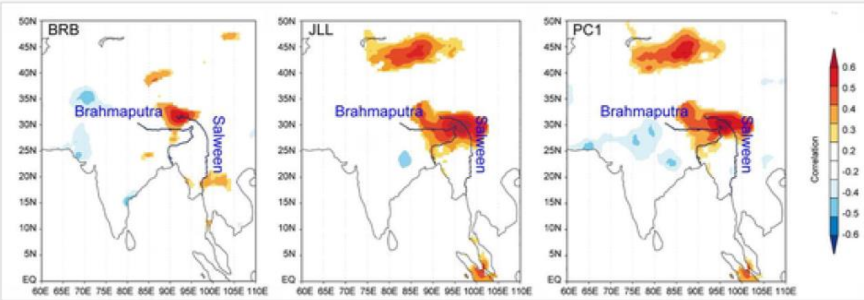

Spatial correlation fields of BRR, JLL and PC1 with regional gridded precipitation of CRU dataset (Harris et al., 2014) for the common periods.

Figure 8

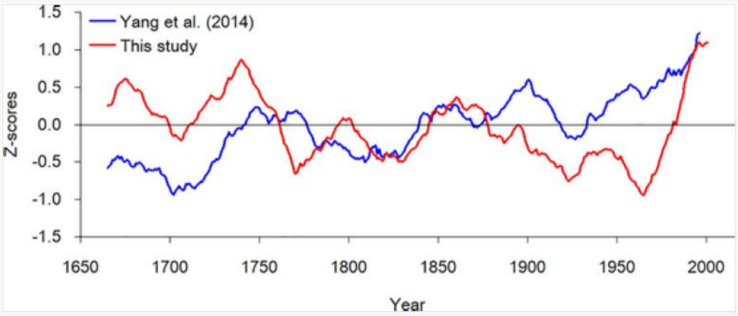

Comparison between PC1 and northern TP precipitation reconstruction by Yang et al. (2014b). The series were adjusted for their long-term averages over period 1650–2010, and smoothed with a 31-year moving average to emphasize long-term fluctuations.